372767

Optical Fuel Injector Patternation Measurements in Advanced Liquid-Fueled, High Pressure, Gas Turbine Combustors

R. J. Locke* *Aeropropulsion Systems Department, NYMA, Inc., Brook Park, Ohio 44142*

Y. R. Hicks, R. C. Anderson, and M. M. Zaller *NASA Lewis Research Center, Cleveland, Ohio 44135*

Abstract — Planar laser-induced fluorescence (PLIF) imaging and planar Mie scattering are used to examine the fuel distribution pattern (patternation) for advanced fuel injector concepts in kerosene burning, high pressure gas turbine combustors. Three fuel injector concepts for aerospace applications were investigated under a broad range of operating conditions. Fuel PLIF patternation results are contrasted with those obtained by planar Mie scattering. For one injector, further comparison is also made with data obtained through phase Doppler measurements. Differences in spray patterns for diverse conditions and fuel injector configurations are readily discernible. An examination of the data has shown that a direct determination of the fuel spray angle at realistic conditions is also possible. The results obtained in this study demonstrate the applicability and usefulness of these nonintrusive optical techniques for investigating fuel spray patternation under actual combustor conditions.

Keywords: Nonintrusive Optical Diagnostics, Planar laser-Induced Fluorescence, Spray Patternation

INTRODUCTION

The abatement of pollutants generated by liquid-fueled gas turbine combustors is increasingly becoming a major issue to government agencies and industries faced with meeting new and impending environmental restrictions and regulations. Essential to meeting these demands, and of critical concern in the design of advanced high pressure liquid-fueled combustors and fuel injectors, is a detailed understanding of the fuel/air mixing process, droplet size and velocity distribution, and fuel density distribution pattern (patternation) encountered in these high pressure combustor concepts. Current diagnostic methods are inadequate to address these issues in the complex flowfields and harsh conditions encountered in present

day combustors. Future designs present even greater obstacles with mass flows expected to reach nearly 200 lb/s and pressure ratios ranging from 60:1 to 100:1. Recent advances in laser technology and optical diagnostic techniques (Taylor, 1993; Rothe and Andresen, 1997) have provided the tools, and the latest window technology (Hicks, *et al.*, 1995) has provided the capability to explore this previously inaccessible and harsh environment.

Until recently, actual combustor flowfields were inaccessible to highly sensitive and specific optical probing techniques. Most previous optical measurements were accomplished using simple gaseous flames at atmospheric (Hanson, 1986) or low pressure (Williams and Fleming 1994). Only recently have investigations been conducted at higher pressure (Battles and Hanson, 1995) but these have been limited to approximately 1.01 MPa and were restricted to simple gaseous fuels. Later experiments were performed with simple liquid fuels in flames approaching 1.01 MPa (Allen *et al.*, 1995), and in internal combustion engines near 2.03 MPa (Andresen *et al.*, 1990). More recently, optical probing of simple gaseous flames, but at greatly elevated pressures near 6.08 MPa (Davidson *et al.*, 1996) have met with some success. To elucidate liquid spray behavior, previous PLIF studies employed exciplex fluorescence techniques (Melton and Verdieck, 1984) but have limited application due to restrictions imposed by temperature limitations and the quenching of the excited state complex by molecular oxygen. Other studies incorporated variants of both PLIF and PDPA (McDonnell *et al.*, 1995) in which a liquid spray, comprised of methanol doped with fluorescein was examined for patternation but these experiments were executed under non-combusting, atmospheric pressure conditions. Only very recently have experiments been implemented which utilize thin film window cooling technology that allows nonintrusive diagnostics to probe and observe in real-time, actual combustor environments with kerosene-based fuels at pressures and temperatures approaching 1.5 MPa and 2000 K respectively (Locke *et al.*, 1996; Locke *et al.*, 1996).

Efforts are underway at NASA Lewis to integrate a number of advanced diagnostic methods to study the performance of next generation combustors and combustor subcomponents. In this study, PLIF imaging of fuel and planar Mie scattering from fuel droplets are used to examine the fuel patternation resultant from advanced fuel injector concepts for liquid fuel burning, high pressure gas turbine combustors for aerospace applications. Three different fuel injector concepts fitted into unique, optically accessible flametubes were investigated. These injectors were examined under a broad range of operating conditions.

A comparison of patternation results is made for each of three different measurement techniques. Differences in spray patterns at different conditions and for distinct fuel injector configurations are readily observable. An examination of the data has also shown that a direct determination of spray angle at realistic conditions is possible. The current study is the first application of the PLIF technique to achieve fuel patternation using a kerosene-based fuel at these extreme conditions of high mass flow, pressure, and temperature. Furthermore, the results obtained in this study demonstrate the applicability and usefulness of non intrusive optical techniques for investigating fuel spray patternation under actual combustor conditions.

EXPERIMENTAL APPARATUS AND PROCEDURES

Facilities

Three different fuel injectors were installed in two unique, optically accessible combustors. The first is a 21.6 cm x 21.6 cm, radially-staged gas turbine combustor or "sector rig", and is designed for testing larger, multi-component, injector systems. The second combustor is a 7.6 cm x 7.6 cm, flametube designed for single component injector testing. Typical rig operating conditions for this series of experiments ranged from inlet temperatures of 533 K - 810 K, inlet pressures of 0.55 MPa - 1.7 MPa (80 psia - 250 psia), and mass flows of 0.32 kg/s - 0.77 kg/s for the flame tube, and 1.13 kg/s - 3.63 kg/s for the sector rig. Equivalence ratios (ϕ) for both combustors ranged from 0.30 to 0.60. The window housings are equipped with UV-grade fused silica windows that measure 3.8 cm axially, 5.1 cm in the cross flow direction, and 1.3 cm thick. To maintain structural integrity at test conditions, the inner surface of the windows is cooled by a thin film of nitrogen, resulting in inner surface window temperatures typically less than 977 K.

The exit plane of each injector projected approximately 6 mm into the window viewing area. The optical detection coordinate system defines x as the azimuthal or horizontal direction with positive x to the right when looking upstream. z is the axial coordinate, with z = 0 at the injector exit plane and positive z in the downstream direction. y is the radial or vertical coordinate with positive values above the rig center or zero point.

Optics and Instrumentation

A Continuum ND 81-C Nd:YAG laser pumping a ND 60 dye laser/UVX ultra-violet wavelength extension system generated the wavelengths necessary for simultaneous measurement of fuel via PLIF and planar Mie

scattering. The 10 Hz, 750 mJ YAG output at 532 nm pumped the dye laser operating with Rhodamine 590 dye, resulting in 190 mJ output at 563 nm. The UVX doubled the dye output to obtain the 281.5 nm UV output, which was maintained at 15 mJ throughout these experiments. A pellin-broca prism separated the doubled dye output from the residual dye fundamental. The bandwidth of the selected wavelength was 1.0 cm^{-1} as measured by a Burleigh UV wavemeter, with pulse widths of 7 ns at full width half maximum (FWHM).

The laser beam transport system, described in detail elsewhere (Hicks *et al.*, 1997) delivered the laser beam to the test cell by a series of remotely controlled, high damage threshold mirrors. Since the UV laser beam has a divergence of only ~5 mrad, it was allowed to freely expand over the full distance of the optical path which ranged from 12 m for the flametube to 25 m for the sector rig. The laser beam was formed into a sheet using a 3000 mm focal length, UV grade cylindrical lens and was directed vertically into the optically accessible combustor. The sheet size at the laser focal volume was approximately 22 mm by 0.3 mm.

Figure 1 illustrates the optical detection setup at the test section The planar fuel fluorescence and planar Mie scattering were collected simultaneously normal to the incident laser sheet using two Princeton Instruments gated and intensified, 16 bit, CCD (ICCD) cameras, each with a 384 x 576 pixel array. The intensifiers, synchronously triggered with the laser pulse, had a gate width of 75 ns. The cameras were equipped with Nikon 105 mm f/4.5 UV Nikor lenses focusing each camera on a plane coinciding with the incident laser sheet passing through the test section center (our defined zero point, or x = 0 position). A computer program was written to coordinate remote positioning of the two cameras and the incident laser sheet. The filters used for collecting the fuel fluorescence comprised a WG-305 glass filter and a narrow band interference filter with a peak transmittance of 16% at 315 nm and a FWHM of 10.6 nm. The Mie scattering was imaged through an interference filter centered at 283 nm with a 2 nm FWHM and transmission of 6%. Due to weak signals, the fluorescence camera's array was binned into blocks of 8 x 8 pixels, effectively reducing the array size to 48 x 72 super-pixels. All images presented here were collected by on-chip averaging the fluorescence or Mie signal on the detector array for fifty laser shots. The incident laser sheet was then traversed across the flow in 1 mm increments from –20 mm to +20 mm about the defined zero point resulting in 41 discrete images for that particular injector and condition.

It was necessary to periodically clean the detector windows during testing of one of the fuel injectors due to a build-up of fuel deposits. This was accomplished by remotely ablating the deposits from both detector windows by sweeping a focused 50 mJ sheet of 532 nm output provided by a Continuum Surelite Nd:YAG laser. The laser insertion window was cleaned by the 281.5 nm incident laser sheet which was scanned continuously over the window's width.

Figure 1 also shows the placement of a two-component Aerometrics Phase/Doppler Particle Analyzer (PDPA) used to measure the light refractively scattered by the fuel droplets (30° forward scatter). Both the transmitter and receiver were aligned 15° from a horizontal plane to maximize the measurement locations accessible within the windowed test section. Transmitting and receiving optic focal lengths were both 500 mm, and the transmitter beam separations were 40 mm. Since the PDPA obtains measurements from a small volume of the flow field, the measurement location was traversed throughout the accessible flow field to characterize the spray. Droplet size distributions, as well as the droplets' axial and tangential velocity components, were acquired by moving the measurement location along the transmitter propagation direction (15° from horizontal). Axial and radial velocity components were measured while traversing 105° from the horizontal.

Image Analysis

A color bar comprising twenty-five colors, plus black (low intensity) and white (high intensity) is used for image analysis purposes. Each color accounts for approximately 10 counts in the linear span from 0 to 255 counts of signal. Black represents the lowest two counts in signal while white represents the highest two signal values. Although the images are corrected for random high noise spikes, they are not corrected for laser sheet energy distribution.

Each image in the subsequent figures shows the fuel patternation from the viewpoint of looking upstream toward the fuel injector (cross flow, or end-on views). These views were obtained by configuring the set of 41 z-y plane images accrued at each test point into a three dimensional array called an image stack. The points between successive images in the stack are interpolated to obtain a smoothed 3-d profile. The resultant image block can then be sliced and observed from any chosen perspective. An example of this process is shown in figure 2. The left hand side of the figure display fuel PLIF images obtained using the

LDI injector assembly fitted into the sector rig. For the purpose of demonstration and for simplicity, only a select few of these z-y plane images are shown. The right hand side of figure 2 shows representative composite cross flow images obtained after implementing this procedure.

All images in each image stack are scaled together so that the highest signal level represents the 99th percentile. Images are displayed in this fashion in order to highlight the lower level structure that would otherwise be lost in the "glare" of other higher intensity features. To eliminate interference attributable to OH fluorescence contributions, all PLIF measurements were accomplished using a non-resonant wavelength, typically 281.5 nm.

RESULTS AND DISCUSSION

Imaging Measurements

Figure 3 shows a comparison of fuel PLIF cross-flow views for the three different fuel injector concepts examined in this study. Each image is scaled independently because they are derived from different injectors and taken at different operating conditions. The left-most two images were acquired using the flametube. The right-hand image was obtained using the radially staged sector combustor. Immediately apparent from the figure is that the left image shows a highly non-uniform fuel distribution, whereas the middle and the right images each display a high degree of symmetry. These images, acquired at the same axial location, approximately 10 mm from their respective injector exit planes, were generated by the previously described computational technique and demonstrate its applicability to diverse experimental conditions and test rig configurations. The crossed white lines in the two left most images denote that particular test rig's center line. These images provide a ready method to display the vast differences between individual fuel injector operating characteristics and performance at design conditions.

A sequence of cross-flow, or end-on, fuel PLIF images is shown in figure 4. The images were obtained for a lean, dual-circuit (pilot and main) fuel injector concept with only the pilot operating, burning JP-8 jet fuel. The injector was installed in the flametube test rig with test conditions of 644 K inlet air, 558 kPa (81 psia) combustor inlet pressure and overall equivalence ratio of 0.445. The five images show the progression downstream from the injector exit plane by the indicated distance increments. These images readily show fuel (dark ring) emerging from the injector (located at z = 0, not shown) in a symmetrical

pattern. Immediately evident from the image is the absence of fuel fluorescence signal at the middle of the injector, denoted by the cross-hairs. Midway from the center in each image, a thick dark mass of fuel is seen to expand as the apparent viewing position moves further downstream (from left to right).

A fortuitous consequence of imaging in this manner is the ability to utilize a simple trigonometric expression and a finely divided ruler to determine the full spray angle for each condition, thus, $\alpha = 2 \tan^{-1} (\Delta h/\Delta z)$, where $\Delta h = \frac{1}{2} (D_{i+1} - D_i)$ is the fuel ring diameter increase as measured from a predetermined position between successive images. Δz is the corresponding axial displacement between these same two images. The spray angle values calculated in this manner agreed well with those determined theoretically. This agreement generally held true throughout these experiments.

Another feature found in this and subsequent images is the slight thickening of the observed fuel ring on the side of the camera acquiring the images, in this case the left hand side. This feature may be attributed to extinction effects, which include incident laser sheet scatter and absorption by fuel droplets, and/or fluorescence trapping. Additionally, the apparent decrease in fluorescence intensity in the last image, z = 12 mm, has two possible causes. The first is the fall off in incident laser sheet energy, solvable by normalizing the images for laser sheet energy distribution. The second cause could be the combustion process consuming the available fuel resulting in a markedly decreased fluorescence level.

Figure 5 presents a sequence of cross-flow planar Mie scattering images obtained for the same injector, but with both pilot and main operating. Test conditions were: 682 K inlet air, 1.6 MPa (232 psia) combustor inlet pressure and overall equivalence ratio of 0.304 . As in the previous figure, the five images progress from left to right, downstream from the injector exit plane by the indicated distance increments. These images, shown in a contour format, distinctly show fuel emerging from the injector (located at z = 0, not shown) in a nearly symmetrical ring formation. Expansion of the fuel ring is again observed in the sequential images from which an accurate fuel spray angle calculation can be made. Noticeably absent from the images in this figure is the Mie scattering from the main. Only the scatter from the pilot is observed. This observation can be explained by reasoning that in this design and at these conditions, the main has greater atomization efficiency than the pilot.

Also in figure 5, the planar Mie scattering intensity is observed to drop off beginning in the z =15 image. This can be attributed to two possible effects. The first, as in the fuel PLIF case, is a fall-off in incident laser sheet energy, which again, could be resolved by normalizing the images for laser sheet energy distribution. The second potential cause is a scarcity of fuel drops in this downstream region due to vaporization.

Figure 6 shows a comparison of simultaneous Fuel PLIF and planar Mie scattering results for the two-circuit fuel injector with both pilot and main operating, burning JP-8 jet fuel. The images, acquired at the same axial location at flow conditions of: T_{inlet} = 682 K, P_{inlet} = 1.6 MPa (232 psia), ϕ = 0.304, demonstrate the significance of comparing these two techniques. Both images display uniform fuel patternation, however, the PLIF image shows two distinct fuel sprays (pilot and main), appearing here as dark rings separated by lighter regions of little or no fuel fluorescence. Conversely, the Mie image exhibits scattering only from the pilot . Since PLIF imaging captures fluorescence from both the liquid and vapor phases of fuel and planar Mie imaging collects scattering only from the liquid, a comparison of the two techniques would be a valuable tool to investigate the fuel vaporization process at real conditions.

PDPA Measurements

PDPA measurements were obtained coincidentally with fuel PLIF and Mie measurements for the two-circuit lean injector concept with only the pilot operating. At each condition, PDPA measurements were attempted across a full diameter of the flow field. When a full traverse was impossible due to optical or time constraints, half of the flow field diameter was characterized. Approximately 8000 droplets were measured at each location. The fuel PLIF images for this injector exhibited a high degree of symmetry, so it was assumed that a single diameter was representative of the spray for that axial location. Despite the use of a focused, frequency-doubled Nd:YAG light sheet to maintain optical access during the tests, only a few points were measured at the lowest inlet air temperature condition due to the accumulation of fuel deposits on the combustor windows. Measurements were more successful at mid-range inlet temperatures, with 60-90% of the droplet measurement attempts typically passing the software validation criteria.

Figure 7 shows the imaged results for this injector fitted into the flametube test rig, acquired simultaneously at approximately 1.27 cm downstream of the injector exit plane, by fuel PLIF and Mie

scattering. The white lines at -15° and -105° show the paths along which PDPA mass flux data was obtained. Figure 7 also presents a drop graph that plots the normalized signals from each of the three techniques. The PDPA data along the -15° line is indicated by solid symbols whereas the corresponding data along the -105° line is shown by the open symbols. It is immediately clear that there is close agreement between the results for the 3 different mass flux measurements along the -105° line. Along the longer -15° line a close agreement is seen on the positive x-axis; however, along the negative x-axis the PDPA data virtually falls off to zero between x = -5 mm and x = -20 mm. This reduction in data rate is attributed to obscuration of the PDPA receiver, which has been observed in high pressure vaporizing sprays (Zaller and Klem, 1994).

In general, there is excellent agreement between the fuel PLIF, Mie scattering and PDPA data for this injector. There appears to be a slight shift of approximately 1 mm along the positive x-axis in the imaged data with respect to the PDPA data. However, this offset is insignificant when considering that each measurement system was installed individually and was independently aligned. Future work will incorporate a single device which will allow repeatable and coincident alignment of each diagnostic technique, thereby achieving the same zero position.

SUMMARY AND CONCLUSIONS

This study has presented images depicting the fuel patternation of lean burning injector concepts operating at conditions of high pressure and temperature. These images, obtained by simultaneous application of PLIF and planar Mie scattering diagnostic techniques, demonstrate the versatility of the image stacking technique to achieve cross-flow views. Using this technique we are able to view upstream and analyze individual fuel injector performance. Fuel PLIF imaged both liquid and vapor fuel but is incapable of distinguishing between the two. The planar Mie scattering images denoted the region in the flowfield where liquid was present. The simultaneous application of these techniques provide complimentary methods to plot liquid fuel patternation. This study indicates that further application of simultaneous fuel PLIF and planar Mie scattering could prove valuable in the study of the fuel vaporization processes at actual combustor conditions.

Comparison of the imaged results with those acquired from PDPA measurements showed a close agreement in trends among the three independent measurement techniques. This observation can be used in future work to develop a procedure to correlate the data obtained from one technique with that from another. In this manner, qualitative image data can be "quantified" by using the quantitative PDPA mass flux data as a reference measurement.

Studies are underway to institute image corrections for incident laser sheet inhomogeneities similar to those recently reported for gaseous-fueled, atmospheric pressure flames (Georgiev and Alden, 1997). However, obstacles not encountered by bench top atmospheric pressure flames must first be surmounted. These impediments include inaccessibility during testing, and the fact that incident laser sheet insertion and all diagnostics must occur through windows of questionable transparency due to the potential accumulation of flow field depositions with some injector designs at certain inlet conditions.

For the imaging work, no attempts were made to address extinction effects attributable to laser sheet scatter or non-resonant absorption by the droplets. Although this is only an issue at the lower inlet temperature conditions where there exists a significant concentration of fuel droplets and the effects appeared minimal in this study, extinction effects pose a significant challenge to applications of this diagnostic technique for this and future higher pressure venues and must be investigated more thoroughly.

REFERENCES

Allen, M., McManus, K., and Sonnnenfroh, D., (1995), PLIF Imaging Spray Flame Combustors at Elevated Pressure, *AIAA Paper* No. 95-0172, 33rd Aerospace Sciences Meeting and Exhibit.

Andresen, P. Meijer, G., Schluter, H., Voges, H., Koch, A., Hentschel, W., Oppermann, W., and Rothe, E., (1996), Fluorescence Imaging Inside an Internal Combustion Engine using Tunable Excimer Lasers, *Appl. Opt.*, **29**, 2392.

Battles, B. and Hanson, R., (1995), Laser-Induced Fluorescence Measurements of NO and OH Mole Fraction in Fuel-Lean, High-Pressure (1-10 atm) Methane Flames: Fluorescence Modeling and Experimental Validation, *J. Quant. Spectrosc. Radiat. Transfer* **54**, 521.

Davidson, D., Roehrig, M., Peterson, E., Di Rosa, M., and Hanson, R., (1996), Measurements of the OH A-X (0,0) 306 nm Absorption Bandhead at 60 atm and 1735 K, *J. Quant. Spectrosc. Radiat. Transfer*, **55**, 755.

Georgiev, N. and Alden, M., (1997), Two-Dimensional Imaging of Flame Species Using Two-Photon Laser-Induced Fluorescence, *Appl. Spectrosc.*, **51**, 1229.

Hanson, R.K., (1986), Combustion Diagnostics: Planar Imaging techniques, *Proceedings of the Twenty-First Symposium (International) on Combustion*, The Combustion Institute, p. 1677.

Hicks, Y., Locke, R., Wey, C., and Bianco, J., (1995), A Unique, Optically Accessible Flametube Facility for Lean Combustor Studies, AIAA Paper No. 95-2685, 31st AIAA/ASME/SAE/ASEE Joint Propulsion Conference and Exhibit, San Diego, CA.

Hicks, Y., Locke, R., Anderson, R., Zaller, M., and Schock, H., (1997), Imaging Fluorescent Combustion Species in Gas Turbine Flame Tubes: On Complexities in Real Systems, AIAA Paper No. 97-2837, 33rd AIAA/ASME/SAE/ASEE Joint Propulsion Conference..

Klassen, M., Thomsen, D., Reisel, J., and Laurendeau, N., (1995), Laser-Induced Fluorescence Measurements of Nitric Oxide Formation in High-Pressure Premixed Methane Flames, *Combust. Sci. and Tech.*, Vols., **110-111**, 229..

Locke, R., Hicks, Y., Anderson, R., and Ockunzzi, K., (1996), OH Imaging in a Lean Burning High-Pressure Combustor, *AIAA Journal*, **34**, 622.

Locke, R., Hicks, Y., Anderson, R., Ockunzzi, K., and Schock, H., (1996), Imaging of Combustion Species in a Radially-Staged Gas Turbine Combustor. *Proceedings of the 33rd JANNAF Combustion Subcommittee Meeting*, CPIA Publication 653, Vol 1, p. 11.

McDonnell, V., Lee, S., and Samuelson, S., (1995), Interpretation of Spray Behavior in Complex Aerodynamic Flows Using Phase Doppler interferometry and Planar Liquid Laser Induced Fluorescence," in S. S. Cha and J. D. Trollinger, (Eds.), *Optical Techniques in Fluid, Thermal, and Combustion Flow*, Proc. SPIE **2546**, 530.

Melton, L. and Verdieck, J., (1984), Vapor/Liquid Visualization in Fuel Sprays, *Proceedings of the Twentieth Symposium (International) on Combustion*, The Combustion Institute, p. 1283.

Rothe, E. and Andresen, P., (1997), Application of Tunable Excimer Lasers to Combustion Diagnostics: A Review, *App. Opt.*, **36**, 3971.

Taylor, A. M. K. P. (Eds.), (1993). For Review see, *Instrumentation for Flows and Combustion*, Academic Press, San Diego, California.

Williams, B. and Fleming, J., (1994), Comparative Species Concentrations in CH_4/O_2/AR Flames Doped with N_2O, NO, and NO_2, *Combust. Flame*, **98**, 93.

Zaller, M. and Klem, M.D., (1994), Shear Coaxial Injector Cryogenic Spray Characterization, in R.J. Richmond and S.T. Wu, (Eds.), *Advanced Earth-to-Orbit Propulsion Technology - 1994*, Vol. 2, NASA CP-3282, p. 194.

Optical Diagnostic Setup

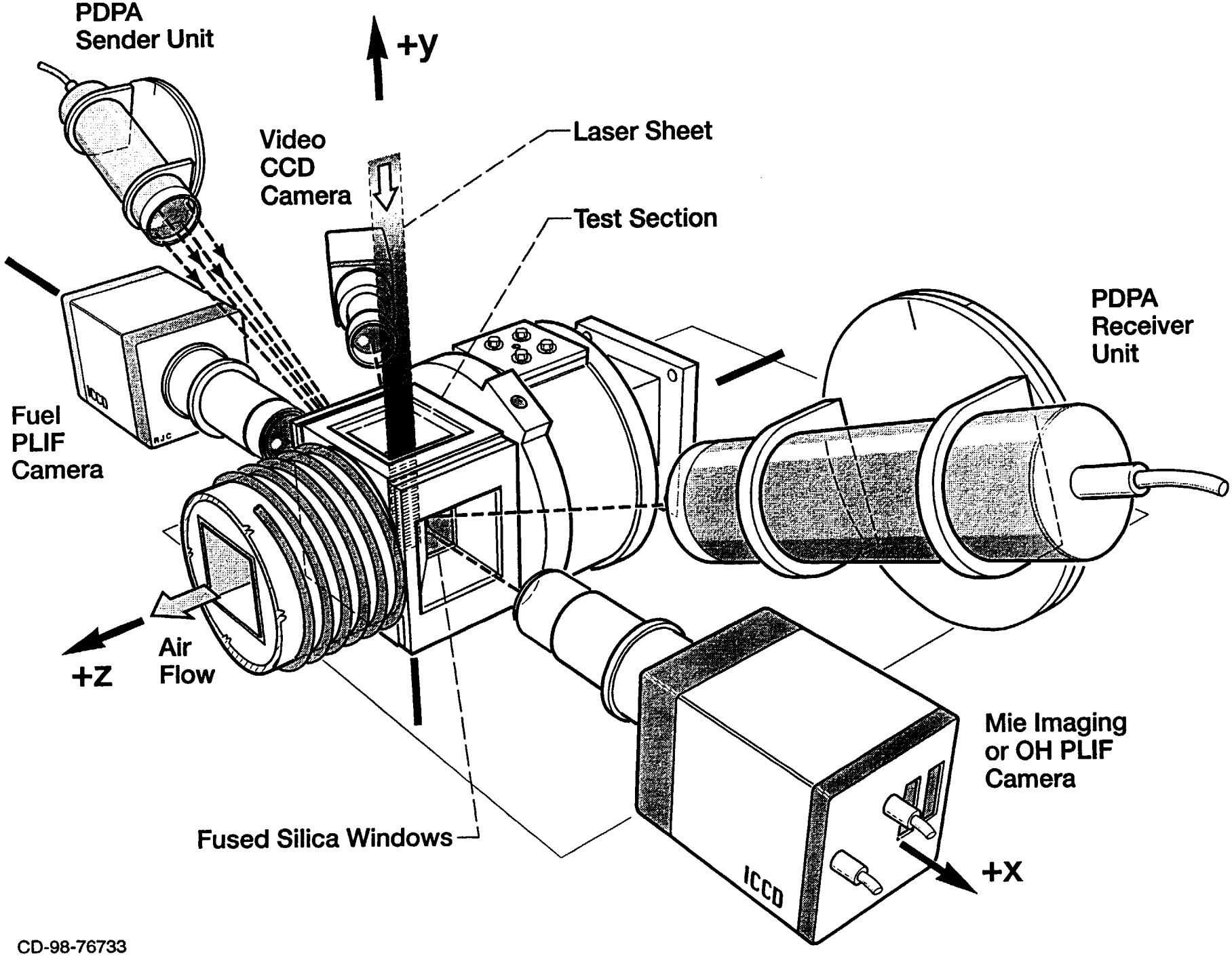

CD-98-76733

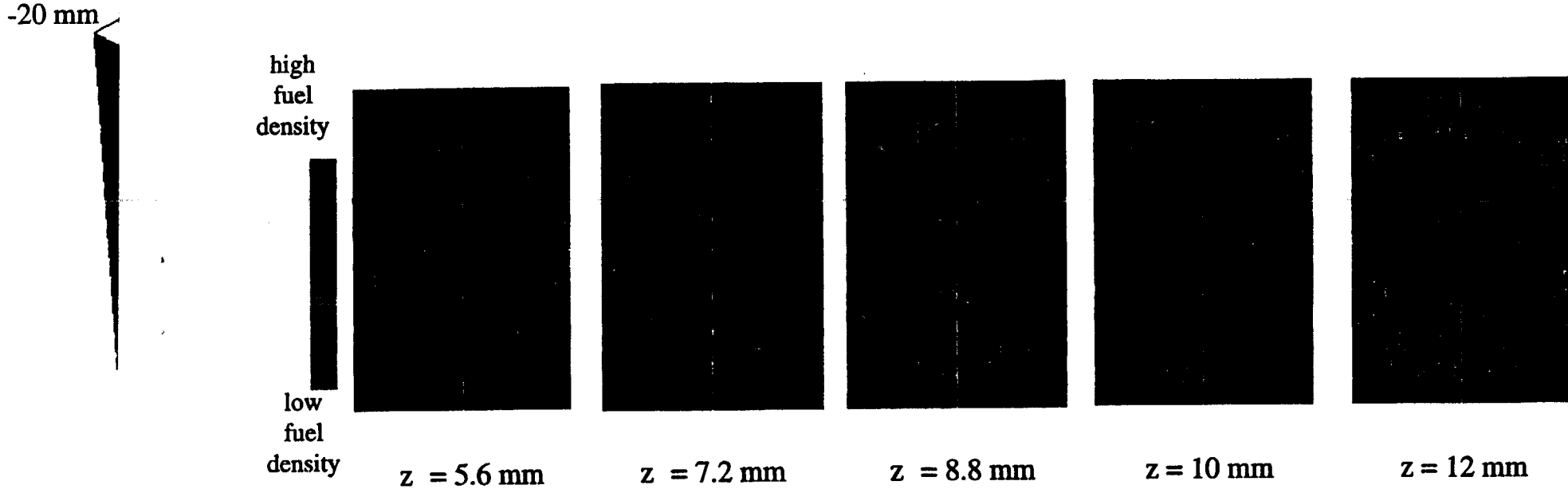
-20 mm
high fuel density
low fuel density
z = 5.6 mm
z = 7.2 mm
z = 8.8 mm
z = 10 mm
z = 12 mm

Se

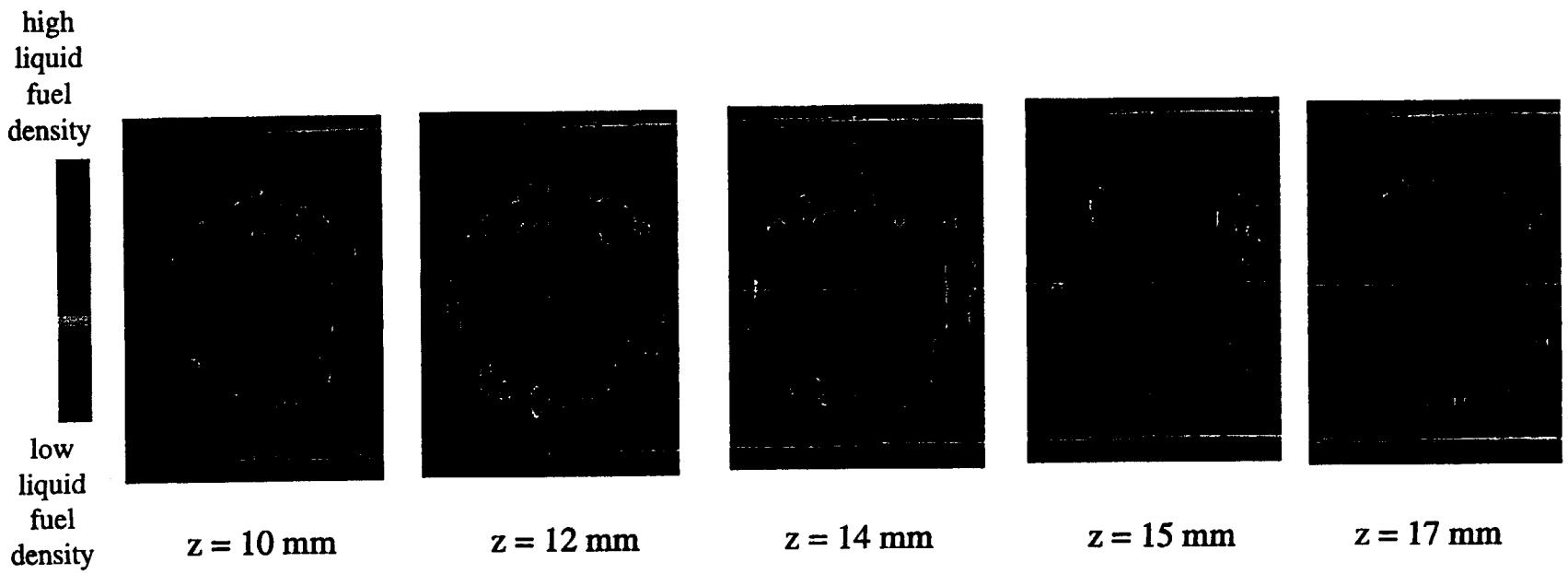
high
liquid
fuel
density
low
liquid
fuel
density
z = 10 mm
z = 12 mm
z = 14 mm
z = 15 mm
z = 17 mm

fig 6

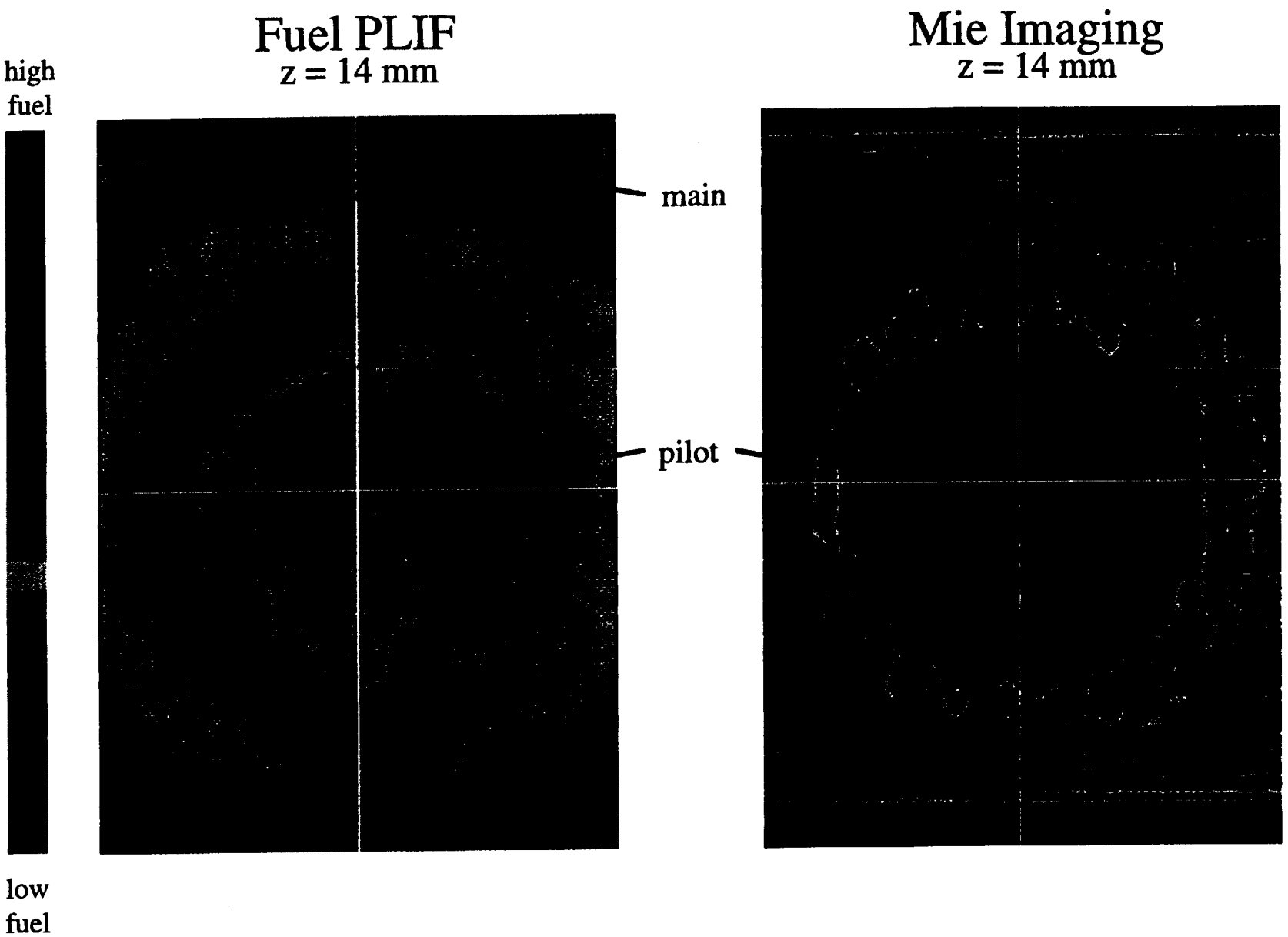
Fuel PLIF
z = 14 mm
Mie Imaging
z = 14 mm
high
fuel
low
fuel
main
pilot

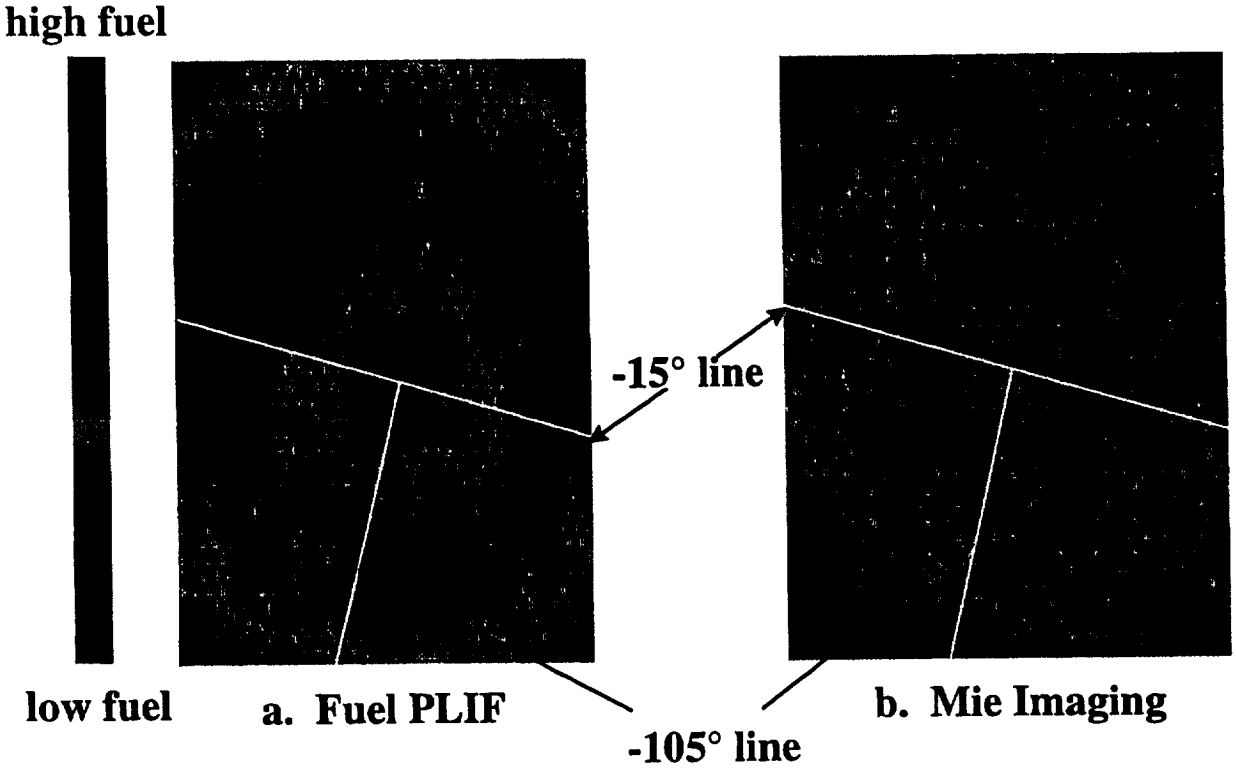

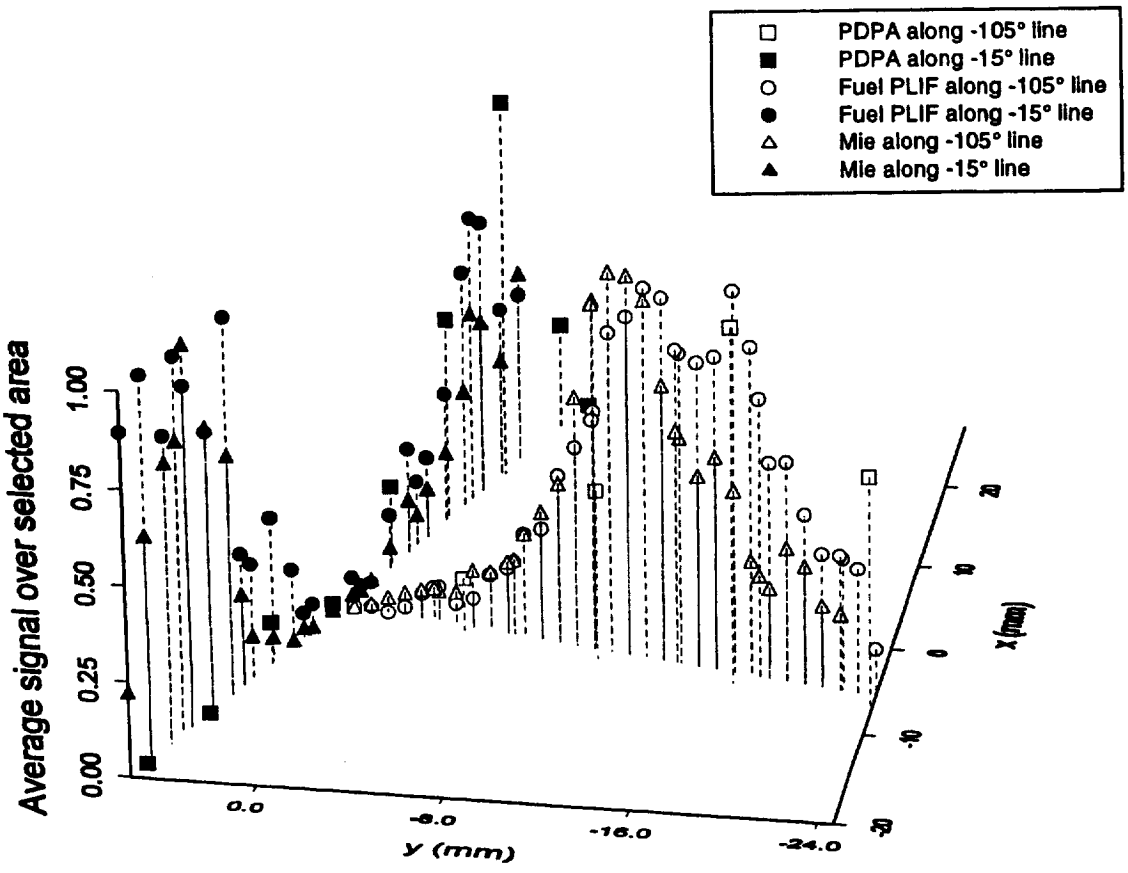

c. 3-d drop-line plot

Figure Captions:

Figure 1. Experimental setup for simultaneous PLIF and Mie imaging, and PDPA analysis.

Figure 2. Example of image stacking of sequential z-y plane fuel PLIF images taken in 1 mm increments across the combustion flowfield to obtain cross-flow (X-Y plane) views. The injector was installed in the radially-staged sector rig. Test conditions are: λ = 281.5 nm, T_{inlet} = 527° C, T_{inlet} = 1.46 MPa, Φ = 0.42. Flow is from left to right.

Figure 3. Fuel patternation via PLIF approximately 10 mm downstream from three lean-burning injector concepts for low emissions combustors. Flow is out of the page.

Figure 4. Sequential cross-flow fuel PLIF images obtained in a combusting flow displaying resultant patternation for two-circuit injector with only the pilot operating. The z dimension gives the distance from the fuel injector dome exit plane. The crossed lines demark the defined injector center point. Test conditions are: λ = 281.5 nm, T_3 = 371°C, P_{inlet} = 0.56 MPa, Φ = 0.445.

Figure 5. Sequential cross-flow planar Mie scattering images obtained in a combusting flow displaying resultant liquid fuel patternation for two-circuit fuel injection. Note the absence of scattering from the outer fuel circuit. Test conditions are: λ = 281.5 nm, T_{inlet} = 419°C, P_{inlet} = 1.6 MPa, Φ = 0.304.

Figure 6. Comparison of simultaneous planar Mie and Fuel PLIF images acquired at the same axial location for a two-circuit fuel injector with both circuits operating. The lack of scattering from the outer circuit in the Mie image reveals that at this position, the effluent is vapor whereas the inner circuit effluent is still a liquid. Test conditions are: λ = 281.5 nm, T_{inlet} = 409°C, P_{inlet} = 1.6 MPa, Φ = 0.304.

Figure 7. Plotted comparison of fuel volume distribution as measured by PLIF, planar Mie scattering, and PDPA. All data was acquired at the same axial location of 1.27 cm from the fuel injector dome exit plane. White lines overlaying the images data denote the path along which PDPA measurements were made. Flow conditions were: λ = 281.5 nm, T_{inlet} = 343, P_{inlet} = 0.56 MPa, Φ = 0.445.